Journal of Thermal Analysis and Calorimetry, Vol. 72 (2003) 253–261

INFLUENCE OF PRECURSOR ON THE THERMALLY INDUCED SYNTHESIS DYSPROSIUM MANGANITE WITH PEROVSKITE STRUCTURE

O. Carp[1*], *L. Patron*[1], *A. Ianculescu*[2], *D. Crisan*[1], *N. Dragan*[1] *and R. Olar*[3]

[1]I. G. Murgulescu Institute of Physical Chemistry, Spl. Independentei 202, Sect. 6, 77208 Bucharest, Romania
[2]Paul Sabatier University, Laboratoire de Chimie des Matériaux Inorganiques et Energétiques, 118 Route de Narbonne, 31062 Toulouse Cedex 4, France
[3]Department of Inorganic Chemistry, University of Bucharest, Panduri 90–92 Street, Sect. 6, 71267 Bucharest, Romania

Abstract

The thermal behaviour of two coordination compounds $[MnDy(malic)_3]\cdot 5H_2O$ and $[MnDy(gluconic)_3]\cdot 12H_2O$ has been studied to evaluate their suitability for dysprosium manganese perovskite synthesis. A decomposition scheme is proposed leading to perovskites with orthorhombic (malic precursor) and hexagonal (gluconic precursor) structures which were obtained after a heating treatment of 4 h at 1000°C with one-hour plateau at 500°C.

Keywords: manganese perovskite, Mn–Dy coordination compounds, thermal behaviour

Introduction

The ability to design technologically useful materials based on chemical principles represents an important goal on the field of materials. An important factor in stabilization of particular structures and/or phases is the synthetic pathway. The observation of giant magnetoresistance phenomenon of the hole-doped perovskite $A_{1-x}A'_xMnO_3$ (A=Ln, A'=Ca^{2+}, Pb^{2+}, Sr^{2+}, Ba^{2+}, Cd^{2+}) [1–4] renewed interest in synthesis routes and properties of nonstoichiometric compounds $LnMnO_{3+\sigma}$ [5–7].

Traditionally they are prepared by ceramic methods [8, 9], but in the last years and low temperatures decomposition synthesis method of various precursors obtained by sol–gel [10–12] or complexation methods are developed [13–16].

The coordination chemistry of lanthanides is characterized by their pronounced tendency to form stable compounds with ligands containing the oxygen donor atom. Thus, the thermal decomposition of polynuclear coordination compounds with carboxylates anions as ligands constitute a viable synthetic route of perovskite synthesis [17–18].

* Author for correspondence: E-mail: carp@apia.ro

1388–6150/2003/ $ 20.00

Akadémiai Kiadó, Budapest
Kluwer Academic Publishers, Dordrecht

In this paper we report the synthesis of dysprosium–manganese perovskite starting from two polynuclear coordination compounds containing as ligands malic and gluconic acids anions. We wish to emphasize the influence of the complexing agent on the thermal behavior of the precursors and implicit mixed oxides properties.

Experimental

The synthesis method represents a modification of that used by Melson and Pickering [19]. The compounds were separated from the reaction medium, a solution containing M^{2+}–Dy^{3+}–polyhydrocarboxylic acid in a molar ratio 1:1:3 (concentrations of metallic salts 0.1 M), by extraction with ethanol. A complete precipitation required 24 h and a constant pH of 5.5–6. The separated compounds were filtered, washed with ethanol and dried. Elemental analysis: the metal content was determined by atomic absorption and gravimetric techniques, and the C, H, N content by a combustion method. By wet chemical redox titration, the average Mn valency in excess of 3+ and equal to 2σ ($DyMnO_{3+\sigma}$) was obtained. The UV-VIS reflectance spectra (11000–54000 cm^{-1}) were recorded with a Jasco V550 device. The IR spectra (4000–400 cm^{-1}) were recorded with a Biorad FTIR 1255 spectrophotometer. Thermal measurements were performed in a Q-1500 Paulik–Paulik–Erdey derivatograph, at heating rates of 2.5–5 K min^{-1} and with sample mass of ~100 mg. X-ray analysis was carried out by means of a Dron 3 X-ray diffractometer with CoK_α radiation. The evaluation of electrical conductivity was made on pellets of ϕ=20 mm and *h*=2–3 mm, using a standard four-point dc technique in the temperature range 30–900°C.

Results and discussion

Synthesis and characterization of the polynuclear coordination compounds

The elemental analysis is in good agreement with the following molecular formulae of the two coordination compounds used as precursor for perovskites:

$$[MnDy(malic)_3]\cdot 5H_2O$$

$$[MnDy(gluconic)_3]\cdot 12H_2O$$

The polyhydroxylic acids are bonded to the metallic ions through their COO^- and C–OH groups (Figs 1 and 2a). This is confirmed by the split of the free carboxylic group band (~1730 cm^{-1}) into two strong bands characteristic for coordinated carboxylic group, namely $\nu_{OCOasym}$~1600 cm^{-1} and ν_{OCOsym}~1390–1400 cm^{-1} and by the shift of the band assigned to $\nu_{(C-OH)}$ to lower frequencies (~1100→1080–1040 cm^{-1}).

The UV-VIS spectra of the two compounds evidenced weak bands due to the spin – forbidden transitions of Mn(II) (d^6)Mn^{2+} in a O_h configuration: $^6A_{1g}\rightarrow{}^4T_{1g}(P)$ $^6A_{1g}\rightarrow{}^4T_{2g}(D)$; $^6A_{1g}\rightarrow{}^4A_{1g}$,$^4E_g(G)$, and $^6A_{1g}\rightarrow{}^4T_{1g}(G)$ at 304, 357, 396 and ~500 nm. Therewith the weak bands due to the transitions from background to excited level of

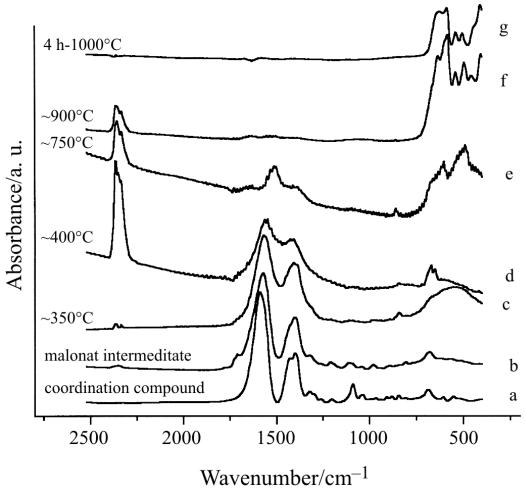

Fig. 1 IR spectra of $[MnDy(malic)_3]\cdot 5H_2O$ coordination compound and its decomposition intermediate

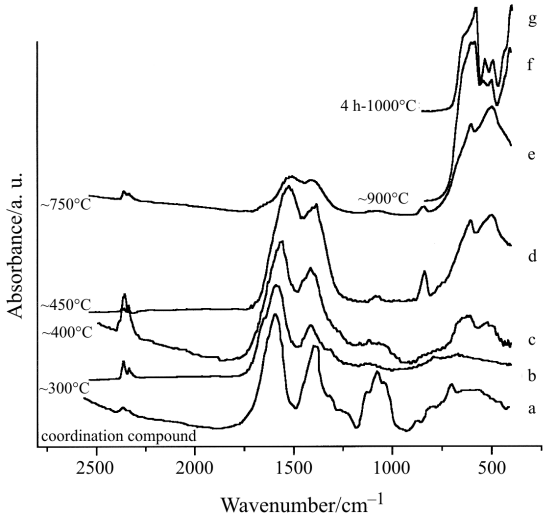

Fig. 2 IR spectra of $[MnDy(gluconic)_3]\cdot 12H_2O$ coordination compound and its decomposition intermediate

4f electrons of Dy^{3+}, (f–f transitions), namely $^6H_{15/2}\rightarrow{}^6F_{3/2}$; $^6H_{15/2}\rightarrow{}^6F_{7/2}$ at ~920 and 1100 nm are identified.

Investigations by thermal analysis

The polynuclear coordination compounds underwent in the temperature range 45–900°C a multistep decomposition (Figs 3 and 4). The non-isothermal analysis

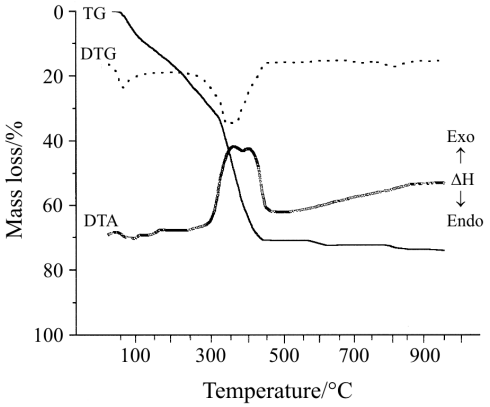

Fig. 3 Thermoanalytical curves (TG, DTG and DTA) of the $[MnDy(malic)_3]\cdot 5H_2O$ coordination compound (heating rate 5° min^{-1}, in air)

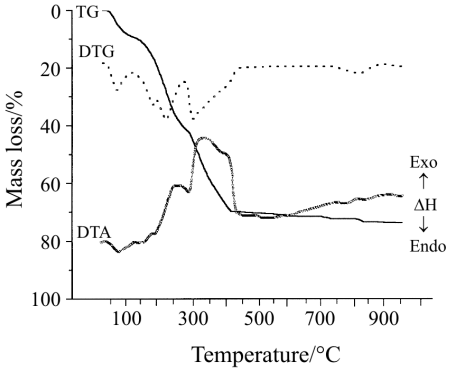

Fig. 4 Thermoanalytical curves (TG, DTG and DTA) of the $[MnDy(gluconic)_3]\cdot 12H_2O$ coordination compound (heating rate 5°C min^{-1}, in air)

was completed by monitoring of solid intermediates by chemical analysis (including determination of manganese average valency) and IR spectroscopy.

Thermal behaviour of $[MnDy(malic)_3]\cdot 5H_2O$

The recorded experimental mass loss is 61.12% in which can be compared with the theoretical value of 62.26% when assuming the solid residue as stoichiometric $DyMnO_3$.

The first decomposition stage (50–231°C) corresponding dehydration (calcd./found 12.68/12.81%) is characterized by two endothermic peaks detected on DTA curve (128 and 169°C). The wide temperature range sustains assumption that, part of the water molecules are coordinated bonded at the metallic ions.

The next decomposition step (231–318°C), associated with a weak exothermic effect, may be assigned to oxidative fragmentation of the malate anion, leading to a malonate intermediate formation [20–21] (calcd./found 12.68/12.13%). The IR spectra (Fig. 1b) evidenced a gradual decrease till disappearance of the band characteristic

to C–OH group (~1080 cm^{-1}) and a shift towards lower frequencies of the ν_{asym} (1588→1571 cm^{-1}). In addition, a band characteristic to free C=O has appeared at ~1710 cm^{-1}, probable due to an incomplete decarboxylation of the malate anion.

The third decomposition region (318–364°C) of mass loss representing the collapse of the carboxylic lattice with $DyMn(CO_3)_{0.5}O_{2.5+\sigma}$ formation (calcd./found 33.55/34.74%), is an overlapping of two decomposition steps. The $\nu_{OCO\ asym}$ shifts to lower frequencies (1566(b)→1571(c)→1555(d) cm^{-1}) and almost overlaps with ν_{sym} which is shifted towards higher frequencies (1404→1416 cm^{-1}). The bands at 841 and 670 cm^{-1} characteristic of carbonates are also noteworthy. A Mn^{4+} content of 61% is found in the decomposition intermediate. At 2630 cm^{-1} a band assigned to $\nu(CO_2)$ is evidenced, suggesting its presence in a trapped state into the solid matrix.

The last two decomposition steps (464–740 and 740–910°C) represent a stepwise decomposition of the oxocarbonates $DyMn(CO_3)_{0.5}O_{2.5+\sigma}$→$DyMn(CO_3)_{0.2}O_{2.8+\sigma}$ (calcd./found 1.82/1.57%)→$DyMnO_{3+\sigma}$ (calcd./found 1.21/1.01%) associated with a decrease in the Mn^{4+} content 61→37→29%. At the end of the thermal decomposition the perovskite lattice is already formed (Fig. 1f).

Thermal behaviour of $[MnDy\ (gluconic)_3]\cdot 12H_2O$

The recorded experimental mass loss value and the theoretical one, assuming the formation of the stoichiometric $DyMnO_3$ as end product, are 72.89 and 73.85%, respectively.

The decomposition starts with two well-defined endothermic processes (41–129 and 129–209°C) corresponding to 5 and 7 molecules of water evolving respectively (calcd./found 8.86/8.00 and 12.40/12.09%). The high temperature range of occurrence of the second process, suggests the existence of coordinated water molecules too.

The second region (209–450°C) of mass loss represents the anion breakdown process with the formation of a $DyMnO_{2.5}CO_3$ intermediate (calcd./found 47.95/49%) in which all manganese is present as Mn^{4+}. The TG/DTG/DTA curves reveal at least three decomposition steps. During the first one (209–293°C) an oxidative fragmentation of the ligand is assumed to take place:

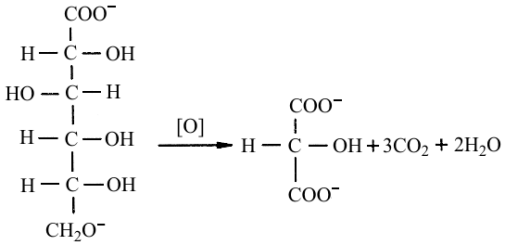

Scheme 1

The thermogravimetric recorded mass loss (calcd./found 25.53/24.57%) and results of elemental analysis (C, H calcd./found 18.90/18.10 and 1.05/0.9%) of the isolated intermediate sustain this assumption. The IR spectra of the isolated intermediate (Fig. 2b)

shows similar absorption bands with the parent compound, but $\nu_{sym\ OCO}$ is shifted by 32 cm^{-1} to higher wavenumbers and the intensity of the bands corresponding to $\nu_{(COH)}$ is decreased. On further heating (293–450°C) the degradation of the above mentioned intermediate is associated (Figs 2c and d) with a shift of $\nu_{asym\ OCO}$ to lower frequencies (1590(b)→1555(c)→1510(d) cm^{-1}) overlapping almost with $\nu_{sym\ OCO}$ band. The entire combination bears resemblance to the principal band of carbonate (~1500 cm^{-1}). The weakly bands at ~850 and ~650 cm^{-1} characteristic to carbonates are also present.

Rising the temperature (450–892°C), leads to the reaction chain

$$DyMnO_{2.5}CO_3 \rightarrow DyMn(CO_3)_{0.5}O_{2.5+\sigma}\ (\text{calcd./found } 1.27/1.31\%) \rightarrow$$
$$DyMn(CO_3)_{0.2}O_{2.8+\sigma}\ (\text{calcd./found } 0.83/0.5\%) \rightarrow$$
$$DyMnO_{3+\sigma}\ (\text{calcd./found } 0.83/0.5\%)$$

conversion and a decrease in Mn^{4+} content as following 100 → 75 → 65 → 57% . The carbonate specific bands decrease in intensity till disappereance with reaction development (Fig. 2e) and the perovskite structure is obtained (Fig. 2f) as the final product.

Characterization of the mixed oxides

The IR spectra reveal that the perovskite structure is already present at the end of the thermal decomposition i.e. before any annealing. From X-ray diffraction point of view the samples are 'amorphous' due to the extremely small particles size. Thus, our investigations concerning the perovskite structures are limited to the oxides obtained after a heating treatment of 4 h at 1000°C with one-hour plateau at 500°C (Fig. 5, Table 1).

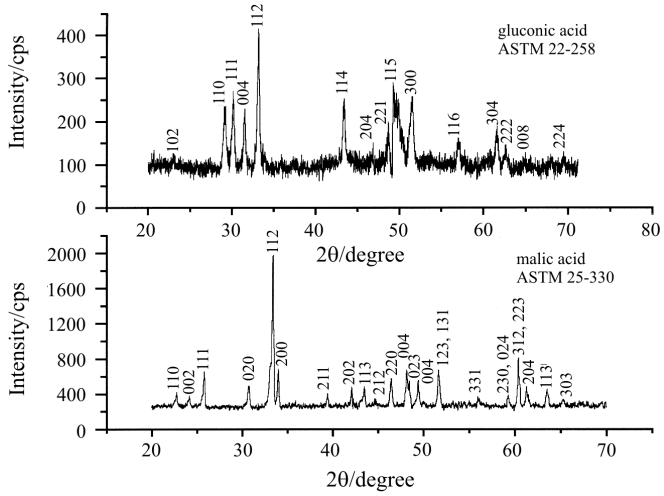

Fig. 5 X-ray diffraction patterns of the oxides generated from the two coordination compounds

The degradation of malic coordination compound generated a perovskite with lower Mn^{4+} (14%) content and orthorhombic structure, due to cooperative ordering of the Jahn–Teller distorted MnO_6 octahedra. The more energetic combustion underwent in the case of the gluconic coordination compound led to a higher Mn^{4+} (20%)

Table 1 Structural characteristics of the $MnDyO_{3+\sigma}$ phase obtained through thermal analysis of the coordination compounds used as precursor

Precursor	Crystallographic system	*a*/Å	*b*/Å	*c*/Å	*V*/Å^3	*D*/Å	10^3<s>	ΔΦ/%
Malic*	orthorhombic	5.2727±0.0005	5.8350±0.0006	7.3880±0.0007	227.23±0.07	630	0.5	8.5
ASTM 22-0330	orthorhombic	5.272	5.795	7.380	225.47	–	–	–
Gluconic**	hexagonal	6.1424±0.0008	–	11.381±0.002	371.9±0.2	703	1.5	5.3
ASTM 22-0258	hexagonal	6.177	–	11.43	377.69	–	–	–

*the estimation has been done using 15 diffraction lines
**the estimation has been done using 8 diffraction lines

content destroying the Jahn–Teller ordering and stabilizing the hexagonal structure. For both oxides, the crystallographic calculations performed with an original program evidenced an even number of diffraction lines (corresponding to the same *hkl*) with a relatively constant intensities ratio, suggesting the coexistence of two crystalline phases characterized by different crystallinity degrees.

The changes in the crystallographic structures of $MnDyO_{3+\sigma}$ with increasing Mn^{4+} concentration are also reflected in the infrared spectra (Figs 1f and 2g). The perovskite structure is characterized by three absorption bands attributed to the stretching (ν_s), bending (ν_b) and lattice (ν_L) vibrations, in the order $\nu_s<\nu_b<\nu_L$. Both ν_s and ν_b would be sensitive to octahedral distortions and the associated lowering of symmetry arising from charge ordering or Jahn–Teller effect, which will determine a splitting of these bands. Thus, we ascribe the doublets present in the range 650–586 and 545–495 cm^{-1} to ν_s and ν_b vibrations, respectively, and the band from 409 cm^{-1} to ν_L *v* one. An increase of the high-frequency side of Mn–O stretching vibrations in the order:

Malic precursor: 636 cm^{-1} (after thermal decomposition)>625 cm^{-1} (after thermal treatment 4 h–1000°C)

Gluconic precursor: 654 cm^{-1} (after thermal decomposition)>648 cm^{-1} (after thermal treatment 4 h–1000°C) indicates an increase in a new raw of Mn–O bond covalency in agreement with Mn^{4+} content progress.

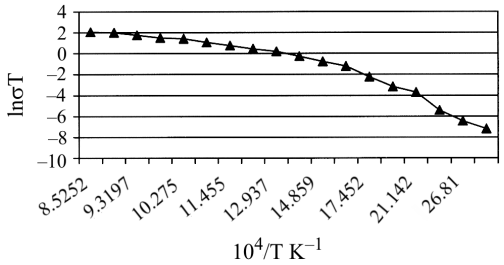

Fig. 6 lnσT–1/T dependency of the malic generated oxide

The electrical conductivity investigations of the oxide generated from malic precursor show a quasilinear lnσT–1/T dependency (Fig. 6). This variation can be understood considering the $Mn^{3+}\rightarrow Mn^{4+}$ electronic transitions, which provide charge carriers according to a small polarons hopping mechanism.

Conclusions

The thermal behaviour of the studied coordination compounds may be summarized by the following sequences:

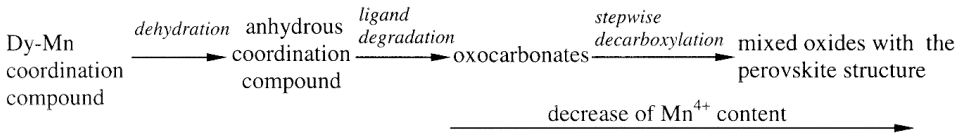

Scheme 2

The ligand degradation represents the decomposition stage which strongly influenced the perovskite structure formation. A higher ligand oxidation capacity leads to a higher Mn^{4+} content in the oxide product, stabilizing a hexagonal structure.

* * *

The financial support by grant 6124 of the Romanian Academy is gratefully acknowledged.

References

1 R. Mahesh, R. Mahendiran, A. K. Raychaudhuri and C. N. Rao, Mat. Res. Bull., 31 (1996) 897.
2 A. Maignan, C. Martin, F. Damay and B. Raveau, Chem. Mater., 10 (1998) 950.
3 S. L. Young, Y. C. Chen, L. Horng, C. C. Chang, H. Z. Chen and J. P. Shi, J. Mag. Mag. Mat., 239 (2002) 11.
4 W. Boujelben, M. Ellouze, A. Cheikhrouhou, J. Pierre and J. C. Joubert, J. Solid State Chem., 162 (2002) 375.
5 R. Manhendiran, S. Tawary, K. Raychaudhuri, T. V. Ramakrishnan, N. Rangarvittal and C. N. R. Rao, Phys. Rev. B., 53 (1996) 3348.
6 J. Töpfer and J. Goodenough, Chem. Mater., 9 (1997) 1467.
7 K. W. Sarathy, P. V. Vanetha, R. Seshadri, A. K. Chetham and C. N. Rao, Chem. Mat., 13 (2001) 707.
8 C. Roy and R. C. Budhani, J. Appl. Phys., 85 (1999) 3124.
9 A. Ianculescu, A. Braileanu, M. Zaharescu, I. Pasuk, E. Chirtop, C. Popescu and E. Segal, J. Therm. Anal. Cal., 64 (2001) 1001.
10 A. Pohl, G. Westen and K. Jansson, Chem. Mat., 14 (2002) 1881.
11 M. C. Gust, L. A. Hamoda, N. D. Evans and M. L. Mecartney, J. Am. Ceram. Soc., 84 (2001) 1087.
12 Z. M. Wang, G. Ni, H. Sang and Y. W. Du, J. Mag. Mag. Mat., 234 (2001) 213.
13 R. Q. Tan, Y. F. Zhu, J. Feng, S. H. Ji and L. Cao, J. Alloy Compds., 337 (2002) 282.
14 H. Aono, M. Tsuzaki, A. Kawauna, M. Sakamoto, E. Traversa and Y. Sadaoka, J. Am. Ceram. Soc., 84 (2001) 969.
15 Y. Masuda, J. Seto, X. Wang and Y. Tuchiya, J. Therm. Anal. Cal., 64 (2001) 1045.
16 O. Carp, L. Patron, A. Ianculescu, J. Pasuk and R. Olar, J. Alloy Compds. (in press 2003).
17 Y. Teraoka, H. Kakebayashi, I. Moriguchi and S. Kagawa, Chem. Lett., (1991) 673.
18 A. González, E. Martínez Tomayo, A. Betrán Porter and V. Cortés Corberán, Catal. Today, 33 (1997) 361.
19 G. A. Melson and W. F. Pickering, Aust. J. Chem., 21 (1968) 1205.
20 V. T. Albu, L. Patron and E. Segal, J. Thermal Anal., 48 (1997) 359.
21 L. Patron, O. Carp, I. Mindru and G. Grasa, J. Therm. Anal. Cal., 55 (1999) 597.